Surface plasmon resonance optical sensor for mercury ion detection by crosslinked chitosan thin film

YAP WING FEN*, W. MAHMOOD MAT YUNUS, MOHD MAAROF MOKSIN, ZAINAL ABIDIN TALIB, NOR AZAH YUSOF[a]
Department of Physics, Faculty of Science, University Putra Malaysia, 43400 UPM Serdang, Selangor, Malaysia
[a]*Department of Chemistry, Faculty of Science, University Putra Malaysia, 43400 UPM Serdang, Selangor, Malaysia*

Mercury ion can be detected by measuring surface plasmon resonance signal with a thin crosslinked chitosan layer deposited on a gold film. The crosslinked chitosan is synthesized by homogeneous reaction of medium molecular weight chitosan in aqueous acetic acid solution with glutaraldehyde as crosslinking agent. By surface plasmon resonance sensor, the optical properties of crosslinked chitosan thin film before and after contacting with different concentration of mercury ion range 0.5 to 100 ppm have been obtained by fitting. The resonance angle shifted higher values to the left as the copper ion concentration increased. By introducing the crosslinked chitosan film, mercury ion detection can be obtained for concentration as low as 500 ppb using surface plasmon resonance technique.

(Received December 20, 2010; accepted March 16, 2011)

Keywords: Surface plasmon resonance, Mercury ion, Crosslinked chitosan

1. Introduction

The increase in industrial and mining activities has caused waterways being polluted with organic and inorganic compounds such as pesticides and heavy metals. Pollution by heavy metal ions, including mercury, has become a major issue throughout many countries due to the possible toxic effects. The exposure of mercury causes loss of myelinated nerve fibers, autonomic dysfunction and abnormal central nervous system cell division. Mercury poisoning has also recently been linked to the neorodevelopmental syndrome and autism. The symptoms of sensory, immune, neurogical, motor and behavioural dysfunction are associated with autism and found in mercury poisoning cases.

Different techniques for mercury ion analysis such as atomic absorption spectroscopy, inductive coupled plasma mass spectroscopy, electrochemical impedance spectroscopy, voltammetry and polarography had been widely used. However, these methods are expensive, complicated sample treatment and mostly take a long measuring period. Optical sensor including surface plasmon resonance spectroscopy is an alternative method for this purpose [1].

Surface plasmon resonance (SPR) spectroscopy is a surface-sensitive technique [2] that has been used to characterize the thickness and refraction index of dielectric medium at noble metal surface [3]. For the last decade, surface plasmon resonance sensors have been extensively studied. Surface plasmon resonance technique has emerged as a powerful technique for a variety of chemical and biological sensor applications [4]. The first chemical sensing based on SPR technique was reported by Liedberg *et al* (1983) [5]. SPR is an optical process in which light satisfying a resonance condition excites a charge-density wave propagating along the interface between a metal and dielectric material by monochromatic and p-polarized light beam [6]. The intensity of the reflected light is reduced at a specific incident angle producing a sharp shadow (called surface plasmon resonance) due to the resonance energy occurs between the incident beam and surface plasmon wave [7]. SPR is regarded as a simple optical technique for surface and interfacial studies and shows the great potential for investigating biomolecules [8]. SPR has been widely demonstrated as an effective optical technique for the study of interfaces and thin films [9]. Compared to the other mercury ion analysis techniques mentioned earlier, SPR spectroscopy has the advantage of size, cost-effectiveness, simple preparation of sample, fast measurement capability and no necessity of reference solution. A high specificity of the SPR optical sensor to heavy metal ions can be obtained by developing or depositing a thin layer of suitable material on gold thin film [10-18].

Chitosan is a copolymer of glucosamine and *N*-acetyl glucosamine linked by β-1,4 glocosidic bonds. Chitosan occurs naturally in some microorganisms, yeast and fungi. It is a non-toxic, biocompatible and biodegradable natural polymer. The commercially available chitosan is mostly derived by alkaline *N*-deacetylation from chitin of crustaceans because it is easily obtained from the shells of crabs, shrimps, lobsters and krill. These two low-cost natural materials had been used for absorption of metal ions, dyes and protein. Compared to chitin, chitosan is more efficient in absorption capacity due to the presence of a large number of amino groups on chitosan chain. However, chitosan is soluble in organic acid, such as acetic acid and formic acid [19].

Crosslinking is an important step to improve the chemical stability of chitosan [20]. One crosslinking agent, glutaraldehyde, is an organic compound with the formula $CH_2(CH_2CHO)_2$. Glutaraldehyde is frequently used in biochemistry applications as an amine-reactive homobifunctional crosslinker.

2. Theory

Surface plasmon wave propagates at the interface of two media with dielectric constant of opposite sign, i.e. metal and dielectric. This surface plasmon wave is a TM-polarized wave (the electric field is parallel to the plane of incidence and perpendicular to the boundary surface between two media while the magnetic field is perpendicular to the plane of incident and parallel to the boundary surface between two media).

The magnitude of electric and magnetic field are related by

$$B = \frac{E}{V} = \frac{n}{c}E = n\sqrt{\varepsilon_0\mu_0}E \tag{1}$$

where

$$c = \frac{1}{\sqrt{\varepsilon_0\mu_0}} \tag{2}$$

Based on Fig. 1 and by using eq. (1) and the boundary conditions, the relationship between the electric and magnetic field can be written as follows:

$$B_a = n_0\sqrt{\varepsilon_0\mu_0}\left(E_0 + E_{r_1}\right) = n_1\sqrt{\varepsilon_0\mu_0}\left(E_{t_1} + E_{i_1}\right) \tag{3}$$
$$B_b = n_1\sqrt{\varepsilon_0\mu_0}\left(E_{i_2} + E_{r_2}\right) = n_2\sqrt{\varepsilon_0\mu_0}E_{t_1} \tag{4}$$
$$E_a = \left(E_0 - E_{r_1}\right)\cos\theta_0 = \left(E_{t_1} - E_{i_1}\right)\cos\theta_{t_1} \tag{5}$$
$$E_b = \left(E_{i_2} - E_{r_2}\right)\cos\theta_{t_1} = E_{t_2}\cos\theta_{t_2} \tag{6}$$

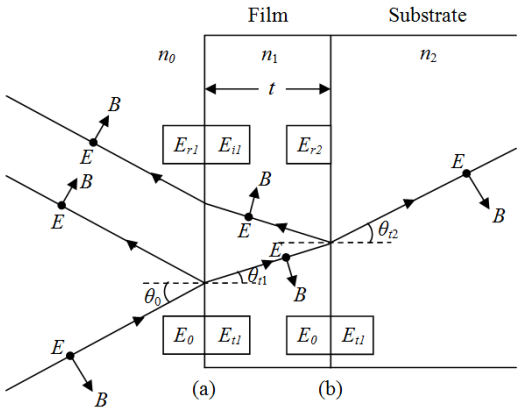

Fig.1. Reflection of a beam from a single layer.

By considering the phase change due to light passing through different layer, i.e.

$$E_{i_1} = E_{r_2}e^{-i\delta}, \quad E_{i_2} = E_{t_1}e^{-i\delta},$$
$$B_{i_1} = B_{r_2}e^{-i\delta}, \quad B_{i_2} = B_{t_1}e^{-i\delta} \tag{7}$$

and using the Euler identities, the relationship between E_1, B_1 and E_2, B_2 are obtained as follows:

$$E_a = (\cos\delta)E_b - \left(\frac{i\sin\delta}{\gamma_1}\right)B_b \tag{8}$$
$$B_a = (-\gamma_1 i\sin\delta)E_b + (\cos\delta)B_b \tag{9}$$

where

$$\tau_1 = \frac{n_1}{\cos\theta_{t_1}}\sqrt{\varepsilon_0\mu_0} \tag{10}$$

Equations (11) and (12) may be written in matrix form as

$$\begin{pmatrix} E_a \\ B_a \end{pmatrix} = \begin{pmatrix} \cos\delta & -i\frac{\sin\delta}{\gamma_1} \\ -i\gamma_1\sin\delta & \cos\delta \end{pmatrix}\begin{pmatrix} E_b \\ B_b \end{pmatrix} \tag{11}$$

Thus, the transfer matrix for single layer is:

$$M_1 = \begin{pmatrix} \cos\delta & -i\frac{\sin\delta}{\gamma_1} \\ -i\gamma_1\sin\delta & \cos\delta \end{pmatrix} \tag{12}$$

where the δ is the phase shift due to the beam passing through different layer, i.e.

$$\delta = \frac{2\pi}{\lambda}tn_1\cos\theta_{t_1} \tag{13}$$

For the case more than one layer, i.e. the boundary (b) substrate replaces by the interface of another thin film, eq. (11) is still valid. E_b and B_b are related to E_c and B_c at the back boundary of the second film layer by a second transfer matrix. Thus, for a multilayer of arbitrary number *N* of layers,

$$\begin{pmatrix} E_a \\ B_a \end{pmatrix} = \prod_{i=1}^{N} M_N \begin{pmatrix} E_N \\ B_N \end{pmatrix} \tag{14}$$

The overall transfer matrix of the film can be represented in general by

$$M_T = \begin{pmatrix} m_{11} & m_{21} \\ m_{12} & m_{22} \end{pmatrix} \tag{15}$$

Based on eqs. (3), (4), (5), (6) and (14), we obtain

$$\begin{pmatrix} \left(E_0 - E_{r_1}\right)\cos\theta_0 \\ n_0\sqrt{\varepsilon_0\mu_0}\left(E_0 + E_{r_1}\right) \end{pmatrix} = \begin{pmatrix} m_{11} & m_{21} \\ m_{12} & m_{22} \end{pmatrix}\begin{pmatrix} E_{t_2}\cos\theta_{t_2} \\ n_2\sqrt{\varepsilon_0\mu_0}E_{t_1} \end{pmatrix} \tag{16}$$

After simpliflying and making use of the reflection coefficient r, defined as

$$r = \frac{E_{r_1}}{E_0} \tag{17}$$

we obtain

$$r = \frac{m_{21}+m_{22}\gamma_2-m_{11}\gamma_0-m_{12}\gamma_2\gamma_0}{m_{21}+m_{22}\gamma_2+m_{11}\gamma_0+m_{12}\gamma_2\gamma_0} \quad (18)$$

Whereby the reflectivity is

$$R = rr^* \quad (19)$$

Hence, a simulation and automatic fitting program had been developed using Matlab based on the matrix method as explained above.

3. Experimental

3.1 Materials

Chitosan with medium molecular weight and degree of deacetylation 75 – 85% was purchased from Sigma Aldrich (St. Louis, MO, USA). Acetic acid and glutaraldehyde were also obtained from Aldrich. Standard solution of mercury with concentration 1000 ppm was purchased from MERCK (Merck, Darmstadt, Germany).

Prism with refractive index, n = 1.7786 at 632.8 nm and the substrate, glass cover slips 24 × 24 mm with thickness 0.13 – 0.16 mm were purchased from Menzel-Glaser.

3.2 Preparation of mercury ion solution

Mercury ion standard solution (1000 ppm) was diluted by using dilution formula ($M_1V_1=M_2V_2$) to produce mercury ion solution with concentration 0.5, 1, 5, 10, 30, 50, 70 and 100 ppm.

3.3 Preparation of chitosan

To prepare chitosan solution, 0.40 g of chitosan was weighed and dissolved in 50 ml 1% acetic acid. The solution was stirred until all the chitosan was dissolved in acetic acid. Then 0.05 g of glutaraldehyde was added to the solution to cross-link chitosan. The resulting solution was stirred thoroughly.

3.4 Preparation of films

The glass cover slips were cleaned using acetone to cleanse off the dirt or remove fingerprint marks laid on the surface of glass slides. Then they were deposited with gold layer using SC7640 Sputter Coater.

Spin coating technique was used to produce a thin layer of crosslinked chitosan film on the top of the gold layer. Approximately 0.55 ml of the solution was placed on the glass cover slip covering the majority of the surface. The glass cover slip were spun at 6000 rev./min for 30 s using Spin Coating System, P-6708D.

3.5 SPR system

Fig. 2 shows the experimental setup for SPR measurement. The SPR measurement had been carried out by measuring the reflected HE-Ne laser beam (632.8 nm, 5 mW) as a function of incident angle. The optical set up consists of a He-Ne laser, an optical stage driven by a stepper motor with a resolution of 0.001° (Newport MM 3000), a light attenuator, a polarizer and an optical chopper (SR 540). The reflected beam was detected by a sensitive photodiode and then processed by the lock-in-amplifier (SR 530).

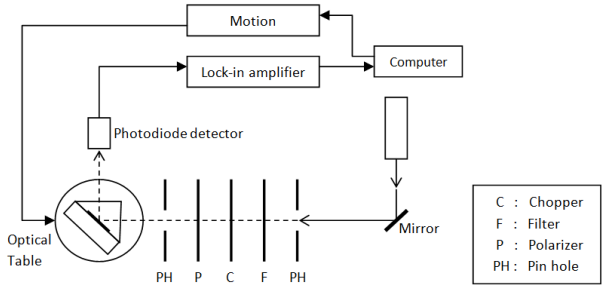

Fig. 2. Experimental setup for angle scan surface plasmon resonance technique.

3.6 Sample cell

A cell was constructed to hold and contact mercury ion solution to glass cover slip with thin films, as shown in Fig. 3. An open-ended brass cylindrical cavity with O-ring seal was attached to glass cover slip, which was attached to the prism by using index matching liquid. The mercury ion solution was filled in the hollow formed so that the laser light contacted to the solution. The prism and the cell were mounted on a rotating plate to control the angle of the incident light.

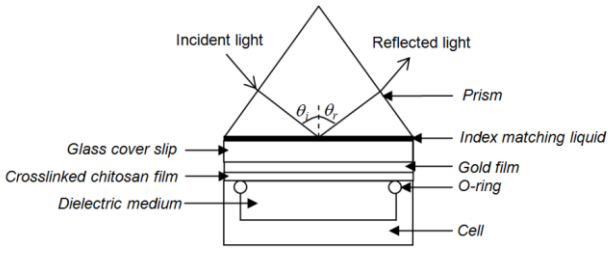

Fig. 3. Structure of the cell for SPR measurement.

4. Results and discussion

Firstly, the preliminary SPR test was carried out for gold film contact with deionised water (single layer) to determine the optical properties of gold layer (the real part refractive index, *n*; the imaginary part of refractive index, *k;* the thickness, *d* of the thin film) and deionised water.

The experimental data and the fitted data are shown in Fig. 4. The optical properties of gold layer were obtained by using the developed Matlab fitting program (matrix method). The values of refractive index, *n* and *k*, for gold layer are (0.190 ± 0.005) and (3.305 ± 0.002) respectively; the thickness, *d* is (46.1 ± 0.1) nm. The refractive index for deionised water is 1.3317. This information is important for the further fitting for multilayer (gold/chitosan film).

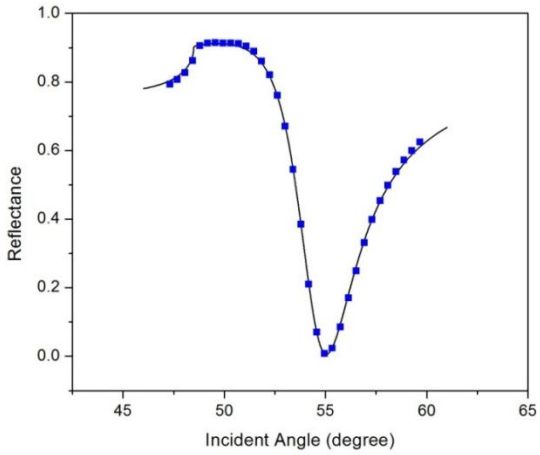

Fig. 4. Fitting experimental data to theoretical data for gold layer in contact with deionised water. The solid line represents the theoretical curve.

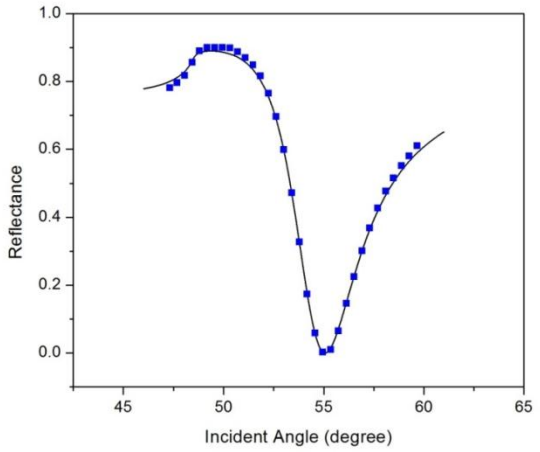

Fig. 5. Fitting experimental data to the theoretical data for gold layer in contact with 100 ppm mercury ion solution. The solid line represents the theoretical curve.

The preliminary SPR test was also carried out for all concentration (range from 0.5 to 1000 ppm) of mercury ion solutions in contact with gold film to determine the refractive index of the solutions. All the results were tabulated in Tables 1 and 2. Fig. 5 shows one typical graph for the experimental SPR curve fitted with theoretical data for gold layer in contact with 100 ppm mercury ion solution. The SPR curves for mercury ion solutions (10 to 1000 ppm) in contact with gold layer were shown in Figs. 6 and 7. From Fig. 7, we can observe that the SPR curves are similar for mercury ion solution below 100 ppm.

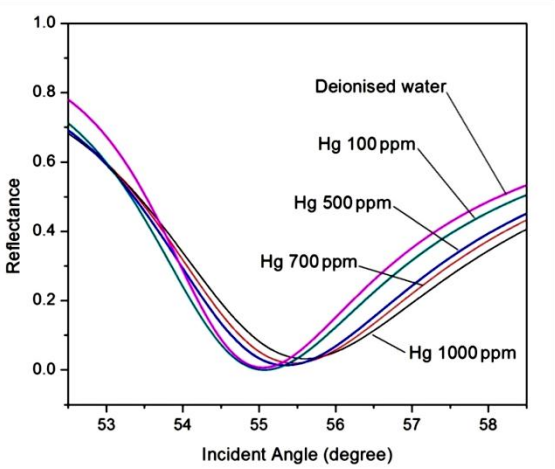

Fig. 6. SPR curves for mercury ion solutions (100 – 1000 ppm) in contact with gold layer.

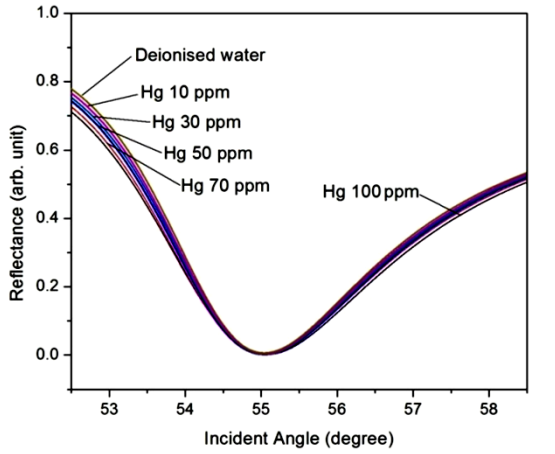

Fig. 7. SPR curves for mercury ion solutions (10 – 100 ppm) in contact with gold layer.

Table 1. The real and imaginary part of refractive index for different concentration of mercury ion solutions after fitting. (0 ppm represents deionised water).

Concentration of mercury ion (ppm)	Real part of refractive index, *n* (± 0.0005)	Imaginary part of refractive index, *k* (± 0.0002)
0	1.3317	0
0.5	1.3317	0.0002
1	1.3317	0.0002
5	1.3317	0.0003
10	1.3317	0.0005
30	1.3318	0.0010
50	1.3318	0.0014
70	1.3318	0.0021
100	1.3321	0.0029
500	1.3359	0.0061
700	1.3374	0.0071
1000	1.3392	0.0089

Table 2. The SPR resonance angle and shift of resonance angle for different concentration of mercury ion solutions in contact with gold layer. (0 ppm represents deionised water)

Concentration of mercury ion (ppm)	Resonance angle, θ_{min} (degree)	Shift of resonance angle, $\Delta\theta$ (degree)
0	55.043	0
0.5	55.043	0
1	55.043	0
5	55.043	0
10	55.043	0
30	55.043	0
50	55.043	0
70	55.043	0
100	55.071	0.028
500	55.350	0.307
700	55.467	0.424
1000	55.601	0.558

Then, the SPR experiment was carried out for gold/crosslinked chitosan film in contact with deionised water. The purpose of this procedure is to determine the optical properties of crosslinked chitosan layer (*n*, *k* and *d*). The experimental data and the fitted data are shown in Fig. 8. Using the multilayer Matlab fitting program, the properties of crosslinked chitosan thin film were determined, where as *n* (1.540 ± 0.005), *k* (0.015 ± 0.002) and *d* (14.0 ± 0.1) nm.

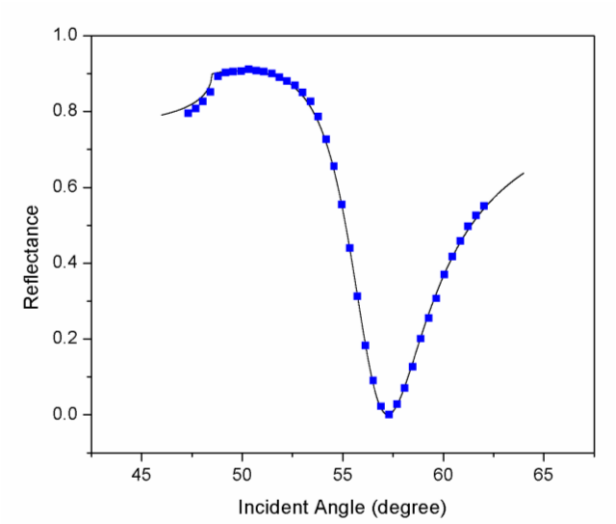

Fig. 8. Fitting experimental data to theoretical data for gold/crosslinked chitosan layer in contact with deionised water. The solid line represents the theoretical curve.

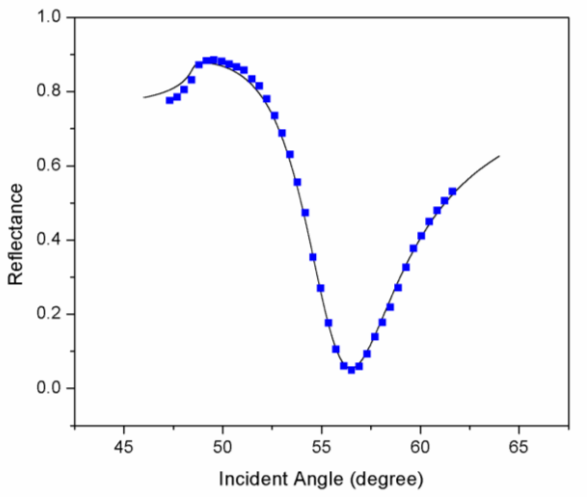

Fig. 9. Fitting experimental data to the theoretical data for gold/crosslinked chitosan layer in contact with 100 ppm mercury ion solution. The solid line represents the theoretical curve.

The SPR experiment was carried out for mercury ion solutions (0.5 to 100 ppm), which was injected one after another into the cell. Each injected solution was left for 10 minutes before the SPR curve was taken. All the fitting results for *n*, *k* and *d* were tabulated in Table 3 while the resonance angle and the shift of resonance angle for all different concentration of mercury ion solution were shown in Table 4. Fig. 9 shows one typical graph for the experimental SPR curve fitted with theoretical data for gold/crosslinked chitosan layer in contact with 100 ppm mercury ion solution. The SPR curves for mercury ion solutions (0.5 to 100 ppm) in contact with gold/crosslinked chitosan layer were shown in Figs. 10 and 11.

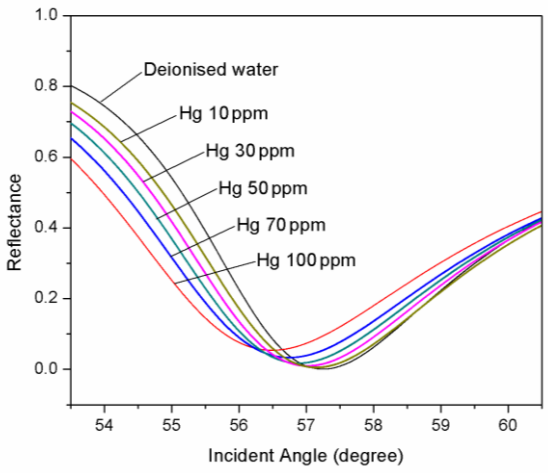

Fig. 10. SPR curves for mercury ion solutions (10 – 100 ppm) in contact with gold/crosslinked chitosan layer.

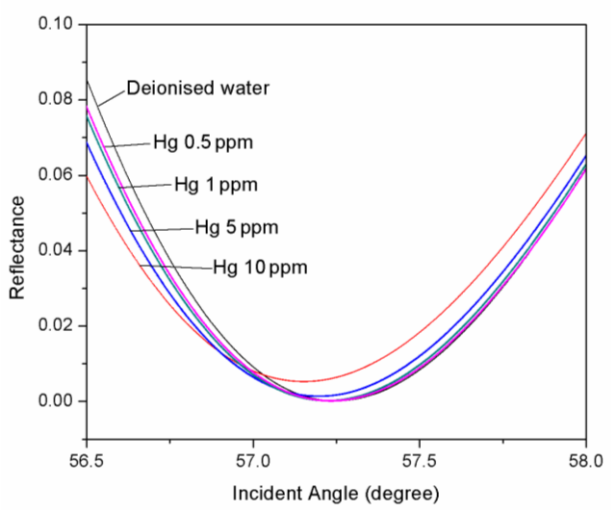

Fig. 11. SPR curves for mercury ion solutions (0.5 – 10 ppm) in contact with gold/crosslinked chitosan layer.

Table 3. The real part of refractive index, the imaginary part of refractive index and the thickness for crosslinked chitosan film after fitting; with different concentration of mercury ion solutions injected into the cell. (0 ppm represents deionised water)

Concentration of mercury ion (ppm)	Real part of refractive index, n (± 0.005)	Imaginary part of refractive index, k (± 0.002)	Thickness of chitosan film, d (± 0.1) nm
0	1.540	0.015	14.0
0.5	1.540	0.020	13.9
1	1.539	0.021	13.9
5	1.538	0.026	13.8
10	1.538	0.036	13.5
30	1.534	0.043	12.8
50	1.533	0.057	12.0
70	1.531	0.077	11.1
100	1.529	0.118	9.2

Table 4. The SPR resonance angle and the shift of resonance angle with different concentration of mercury ion solutions in contact with gold/cross linked chitosan layer. (0 ppm represents deionised water).

Concentration of mercury ion (ppm)	Resonance angle, θ_{min} (degree)	Shift of resonance angle, Δθ (degree)
0	57.248	0
0.5	57.236	0.012
1	57.225	0.023
5	57.192	0.056
10	57.153	0.095
30	57.012	0.236
50	56.885	0.363
70	56.746	0.502
100	56.496	0.752

From the results, as the concentration of mercury ion increased, the value of k for crosslinked chitosan layer increased while the thickness of the crosslinked chitosan layer decreased. Mercury ion may interact with the crosslinked chitosan layer because of the formation of pair between the positive charge from mercury ion and negative charge from amine functional group in chitosan. This may cause the erosion of the sensor system.

In this study, the crosslinked chitosan thin film had an important role in detection of mercury ion had been proved. There were no changes in resonance angle for mercury ion concentration below 100 ppm in contact with gold film only. As the crosslinked chitosan thin film introduced above gold layer, the resonance angle changed obviously and the detection limit for mercury ion is as low as 0.5 ppm. The comparison of the shift of resonance angle for both gold film and gold/crosslinked chitosan film in contact with different concentration of mercury ion was shown in Fig. 12.

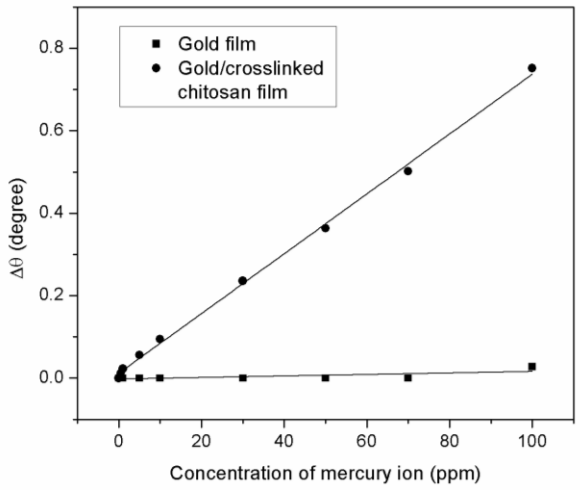

Fig. 12. Comparison of the shift of resonance angle for different concentration of mercury ion in contact with gold film and gold/crosslinked chitosan film.

5. Conclusions

In this work, SPR optical sensor for mercury ion detection had been developed by depositing the crosslinked chitosan thin film onto gold layer. The optical properties of crosslinked chitosan thin film before and after contacting with different concentration of mercury ion range 0 to 100 ppm have been obtained using SPR technique. As the concentration increased from 0 (deionised water) to 100 ppm, the value of k increased while the thickness of the crosslinked chitosan film decreased. This lead to the resonance angle shifted higher values as the mercury ion concentration increased. Besides, the refractive index for different concentration of mercury ion solution were determined by contacting the solution to gold only film. The results also showed that there were no changes in resonance angle for mercury ion concentration below 100 ppm. The crosslinked chitosan

film has increased the sensitivity of the mercury ion detection. The gold/crosslinked chitosan film is highly sensitive for mercury ion with detection limit 500 ppb.

Acknowledgements

The authors would like to thank the Malaysian Government for the fund support through SAGA. The laboratory facilities provided by the Department of Physics, Faculty of Science, University Putra Malaysia, are also acknowledged.

References

[1] J. Homola, S.S. Yee, G. Gauglitz, Review. Sens. Actuators B: Chem. **54,** 3 (1999).
[2] N. J. Tao, S. Boussaad, W. L. Huang, R. A. Arechabalets and J. D'Agnese: Rev. Sci. Instrum. **70,** 4656 (1999).
[3] W. Y. W. Yusmawati, H. P. Chuah, W. M. M. Yunus: American Journal of Applied Science **4**(1), 1 (2007).
[4] H. Q. Zhang, S. Boussaad, N. J. Tao: Rev. Sci. Instrum. **74,** 150 (2003).
[5] B. Liedberg, C. Nylander, I. Lundstrom: Sens. Actuators B: Chem. **4**, 299 (1983).
[6] K. Kurihara, K. Suzuki: Anal. Chem. **74,** 696 (2002).
[7] J. Homola: Surface Plasmon Resonance Based Sensor (Springer, New York, 2006) pg. 45.
[8] C. M. Wu, L. Y. Lin: Sens. Actuators B: Chem **110,** 231 (2005).
[9] J. Mendelez, R. Carr, D. Bartholomew, H. Taneja, S. Yee, C. Jung and C. Furlong: Sens. Actuators B: Chem. **38,** 375 (1997).
[10] S. W. Chah, J. H. Yi and R. N. Zare: Actuators B: Chem. **99** (2004) 216.
[11] C. C. Yu, P. C. Lai and S. Sadeghi: Sens. Actuators B: Chem. **101,** 236 (2004).
[12] Y. T. Zhang, M. T. Xu, Y. J. Wang, F. Toledo, F. M. Zhou: Sens. Actuators B: Chem. **123,** 784 (2007).
[13] J. Moon, T. Kang, S. Oh, S. Hong, J. Yi: Journal of Colloid and Interface Science **298,** 543 (2006).
[14] E.S. Forzani, K. Foley, P. Westerhoff, N. Tao: Sens. Actuators B: Chem. **123,** 82 (2007).
[15] F. Mirkhalaf, D. J. Schiffrin: Journal of Electroanalytical Chem. **484,** 182 (2000).
[16] A. Sugunan, C. Thanachayanont, J. Dutta, J. G. Hilborn: Science & Technology of Advanced Material **6** (2005) 335.
[17] S. M. Lee, S. W. Kang, D. U. Kim: Dyes & Pigments **49,** 109 (2001).
[18] C. M. Wu and L. Y. Lin: Biosensors & Bioelectronics **20**(4), 864 (2004).
[19] C. L. Shauer, M. S. Chen, M. Chatterley, K. Eisemann, E. R. Welsh, R. R Price, P. E. Schoen F. S. Ligler: Thin Solid Films **434** (2003) 250.
[20] D. R. Bhumkar, V. B. Pokharkar: AAPS Pharm. Sci. Tech. **7**(2) (2006) 50.

*Corresponding author: yapwingfen@gmail.com